Design of a brushless rotor supply for a wound rotor synchronous machine for integrated starter generator

Jerome Legranger*†, Guy Friedrich†, Stéphane Vivier†, and Jean Claude Mipo*
* Valeo Electrical System
2, Rue André Boulle / BP150
94017 Créteil Cedex / France
Email: jerome.legranger@utc.fr and jean-claude.mipo@valeo.com
† University of Technology of Compiègne
Electromechanical laboratory / BP20529
60205 Compiègne Cedex / France
Email: guy.friedrich@utc.fr and stephane.viver@utc.fr

***Abstract*— Wound rotor synchronous machines present interesting performances for integrated starter generator. Nevertheless, the lack of reliability of their gliding contacts remains their main drawback. The following paper proposes to replace the gliding contacts of such a wound rotor synchronous machine by an iron silicon axial rotary transformer operating as a contactless transmission power system. The design process is based on an accurate non-linear multidisciplinary analysis model divided into a magnetic, thermal and electrical part, optimized thanks to a sequential quadratic programming algorithm. The method is applied to a particular wound rotor synchronous machine and the electromagnetic and thermal performances are subsequently confirmed using the finite element method (FEM). The optimal result indicates that the rotary transformer is a good challenger to gliding contacts in term of compactness. Other advantages and limitations of the optimal rotary transformer are discussed.**

***Index Terms*— Rotary transformer, multi-domain modelling, synchronous machine, integrated starter generator**

I. Introduction

The study of integrated starter generator (ISG) applications leads to make comparisons between different machines structures : induction machines [1] [2], wound rotor synchronous machines (WRSM) [2] [3], reluctant and permanent magnet machines [4]. All these machines must respect very strong rules and specifications (low length, high torque, high temperature, speed and efficiency).

In this context, the wound rotor synchronous machine [3] owns lots of advantages : low cost rotor (no rare earth permanent magnet), three control variables (id, iq, if) allow new optimization possibilities compared with permanent magnet machines (id, iq). A special design of the rotor minimizes the required field current and allows the use of a rotating transformer if a total brushless configuration is required. Beyond these advantages, it is interesting to note a significant improvement of the safety thanks to the possibility of cancellation of the field current and so, limiting the risks of over voltages for high speed operations. The level of the flux density in the air-gap is limited only by the quality of sheets employed, thus, authorizing significant specific torque.

Moreover, during the generating mode, the converter can be operated in a synchronous rectifier mode, thus, authorizing an increase in the efficiency and a reduction of the electromagnetic disturbances and converter losses by avoiding an operation in the PWM mode [2].

Nevertheless, the rotor supply of the WRSM remains the main drawback of the machine even if specific constraints taken into account in the early stages of an optimal design can lead to a very compact and somewhat reliable system of gliding contacts [3]. These mechanical contacts present indeed a limited lifetime that induces a difficult maintenance for integrated structures, and problems in respect of noise, contact wear, EMI environment and eventually contamination due to wear debris [5].

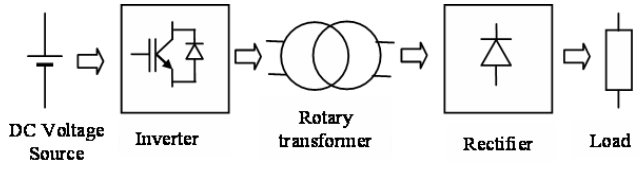

Fig. 1. Typical rotary transformer converter topology

A wise solution consists then in replacing the gliding contacts with contactless transmission systems and particularly with rotary transformers [6]. Rotary transformers are similar to conventional transformers expect that a large airgap between the primary and the secondary is arranged to enable the rotation of a part of the structure.

The purpose of this article is to explore the benefits and limitations of a rotary transformer when applied to the specific WRSM for ISG application described in [3].

In a first part, the basic principles of rotary transformers are recalled. Then, the design tool used for the investigation is presented thoroughly. The software combines a nonlinear multidisciplinary (magnetic, thermal and electrical states) coupled lumped parameter model associated with a classical sequential quadratic programming (SQP) optimization algorithm. Finally, an optimal solution dedicated to the WRSM of [3] is proposed and discussed. This design solution is validated by the finite element method (FEM) both for magnetic and thermal aspects.

II. Basic system structure

The rotary transformer is a part of a DC-DC contactless conversion system (figure 1) that includes :

- a DC voltage source like a battery
- a primary converter : a PWM full bridge inverter or other soft switching structures [8]
- a rotary transformer with a large airgap, generally an axial transformer (figure 2) for our integrated WRSM to ensure both the robustness towards axial misalignment and a small size
- a secondary converter : a rotating bridge rectifier

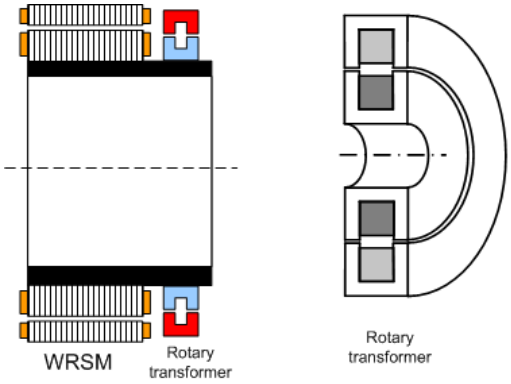

Fig. 2. Cross section of the WRSM and the axial transformer : internal core rotating secondary and external core static primary

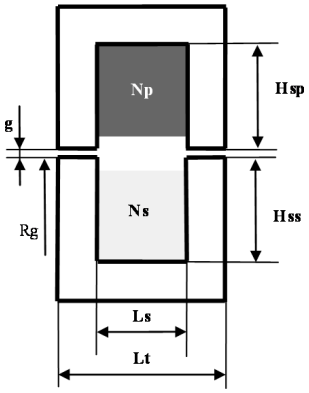

Fig. 3. Determination of the optimization variables for an axial rotary transformer

The axial transformer is located side by side with the WRSM ISG (figure 2). The transformer core is made of iron silicon steel adapted to frequencies below 1 kHz and more robust to mechanical stress than soft ferrites.

III. Formulation of the optimization problem applied to a rotary transformer

The design of a rotary transformer is a non linear, multiphysic and multivariable problem. This complexity leads to adopt an efficient solution research methodology based on an optimization process, typically a sequential quadratic programming algorithm (SQP) [9].

The optimization consists first in the selection of optimization variables OV among all the design variables DV and then to obtain their optimal values OV_{opt} which :

- satisfy the minimization of an objective function f_{obj}
- agree with required constraints

Both the objective function and the constraints are evaluated thanks to an appropriate multiphysic model of the rotary transformer.

A. Choice of the optimization variables

The choice of the optimization variables complies first with the necessity of specifying continuous differentiable variables to suit SQP method requirements, then to perfectly determine the magneto-thermal state of the transformer and finally to have a reasonable computation time.

This leads to distinguish [9] :

- continuous geometric OV : airgap radius R_g, primary and secondary slot length L_s and heights H_{sp} H_{ss}, total length L_t
- discrete electric geometric OV : primary and secondary turns number. These latters do not respect the first rule of SQP optimization and have been treated in two steps : in the first step, these variables have been considered as continuous and in a second step they have been kept constant and an optimization has been performed on the remaining OV.

B. Definition of the objective functions

The aim of our study is to ensure the compactness of the structure that is to say to determine the minimal width of the transformer for fixed internal and external diameters.

Consequently, the objective function is :

$$f_{obj} = \frac{L_t}{L_{normalisation}} \tag{1}$$

where L_t is the total width of the transformer and $L_{normalisation}$ a reference width that normalizes the objective function.

C. Definition of the constraint function

The constraint functions are of five types :

- Geometric constraints
- Thermal constraints
- Magnetic constraints
- Supply constraints
- Efficiency characteristics

1) Geometric constraints: The geometric constraints are mainly related to manufacture requirements. In fact, the width of the yoke leg needs to be at least 3 or 5 mm. The upper and lower parts of the yoke are subject to the same kind of constraints. Besides, the total width has to be minimised length a maximum allowed of 40 mm.

2) Thermal constraints: Thermal constraints first deal with the temperature of the windings that does not exceed the maximum temperature allowable by their thermal class (for instance 180°C for H class). Then, the temperature of the yoke soft magnetic material is limited by Curie temperature to avoid the loss of its magnetic properties.

3) Magnetic constraints: The induction in each part of the secondary and primary yoke is limited to an appropriate induction level depending on the iron silicon sheet quality.

4) Supply constraints: As the transformer is supplied with a battery, the maximum allowable voltage that feeds the primary converter is limited to the battery maximum voltage.

5) Efficiency characteristics: A minimum efficiency of 80% is applied to the transformer (not to the whole DC-DC system). Moreover, the battery current is limited to a maximum value (primary converter switches requirements).

Finally, all the optimization variables are also limited to avoid unrealistic values such as negative lengths.

D. Coupled multiphysic model

The model evaluates at each iteration of the optimization process, the thermal, electrical and magnetic state of the rotary transformer. As a result, the constraints and the objective function are perfectly estimated.

The model adopts a coupled multiphysic structure to take into account the strong link between each state. The only strong hypothesis of the model is that the inverter delivers a sinusoidal voltage (no chopping effect).

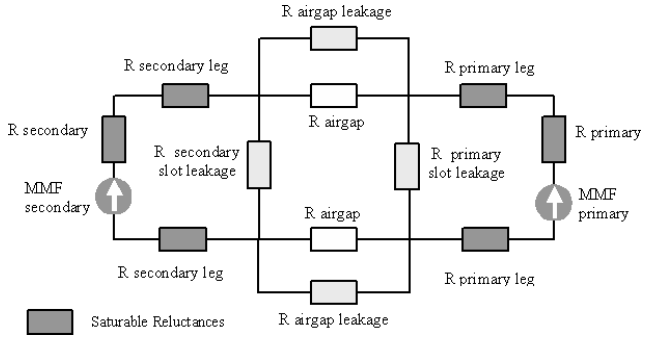

Fig. 4. Reluctant network for the rotary transformer

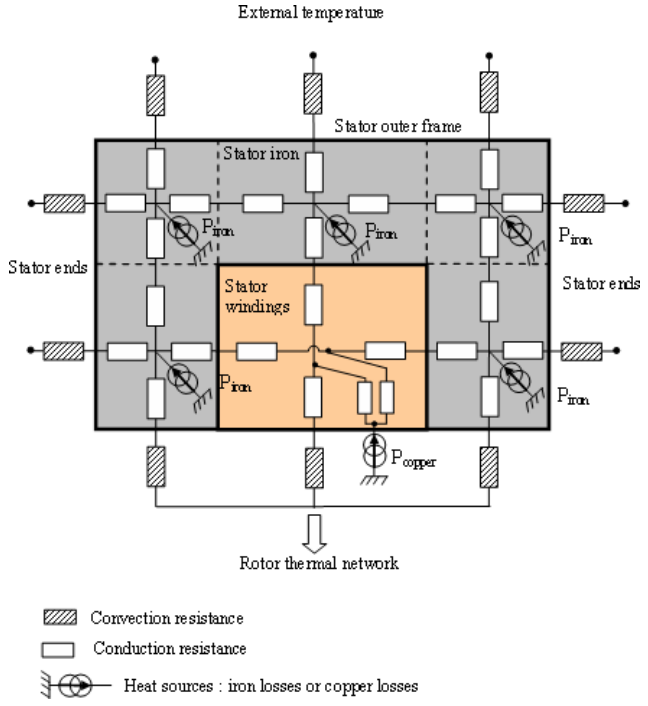

Fig. 5. Two-dimensional thermal network of the rotary transformer stator

1) Magnetic state: The magnetic state of the coaxial transformer is perfectly defined for given temperatures (thermal model) of the windings, and given primary and secondary currents (electric model).

The chosen model is a lumped parameter reluctance network that allows a good compromise between accuracy and computation time.

Saturation of the yoke soft magnetic material is classically taken into account by the Marocco formula and solved thanks to an iterative process [9] based on Newton-Raphson method.

The calculation of the air gap reluctance includes the fringing path according to the heuristic methods given in [10] and [8].

The calculation of the external fringing permeance is performed assuming that the flux line is divided into a straight line and two quarters of circle :

$$R_l = \frac{1}{2\pi\mu_0 \left(\frac{h}{\pi} + \frac{(\pi R_g - g)}{\pi^2} \ln(1 + \frac{\pi h}{g})\right)} \quad (2)$$

where R_g is the airgap radius, g the airgap width, h the yoke height and μ_0 the absolute permeability.

2) Thermal state: The thermal model allows the estimation of the average temperature of the windings and the yoke thanks to a two dimensional steady state lumped parameter network.

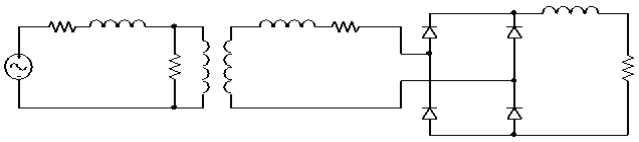

Fig. 6. Electrical model of the rotary transformer stator

The heat transfer sources are copper losses determined in a traditional way and iron losses whose calculation is carried out with standard Bertotti formula [11] assuming that the flux density in the transformer is sinusoidal.

The external air temperature is supposed to be constant and the temperature of the rotor (secondary) internal diameter is fixed to the temperature of the shaft on which the transformer is mounted.

The conduction cells estimation is based on the resolution of the heat transfer equation [12]. The determination of the winding equivalent thermal conductivity encompasses the filling factor effect, the average disposition of the winding in the slot and the number of conductor per slot [13].

The convection cells determination relies on the estimation of convection coefficients with empirical correlations of Churchill and Chu for the stator (primary) outer surface [14] [12] which states that the Nusselt number Nu is :

$$Nu = \left(0.6 + 0.387 \left(\frac{Ra_D}{\left(1 + \left(\frac{0.559}{Pr}\right)^{9/16}\right)^{16/9}}\right)^{1/6}\right)^2 \quad (3)$$

with the Rayleigh number :

$$Ra_D = \frac{g\,\beta\,Pr}{\upsilon^2}\, D_h^3\, (T_{stator} - T_{air}) \quad (4)$$

where g is the gravitational force of attraction (m/s^2), T_{air} and T_{stator} (K) are the temperatures of air and the stator, β the fluid coefficient of cubical expansion (K^{-1}), Pr the Prandtl number and υ the cinematic viscosity (St). These two latter are evaluated at the temperature $(T_{air} + T_{stator})/2$.

Then, with Kreith correlation for the rotor (secondary and smooth discoid rotating surface subject to laminar flow) subjected to forced convection [14] [12] :

$$h_c = 0.35\ \lambda_{air}\ \left(\frac{\omega}{\upsilon}\right)^{1/2} \quad (5)$$

associated with radiation coefficients through Stefan Boltzmann law.

3) Electrical state: As previously described, the primary converter PWM voltage is reduced to its first harmonic (sinusoidal hypothesis). So the maximum amplitude of the primary voltage is equal to the maximum battery voltage minus the voltage drop in the switches.

The computation of the electrical model is based on the electrical system simulation software SimPowerSystem of Matlab to take into account :

- the commutation overlap due to the low primary and secondary coupling factor
- the voltage drop for each element, particularly for low battery voltage of 36V
- the secondary current waveform

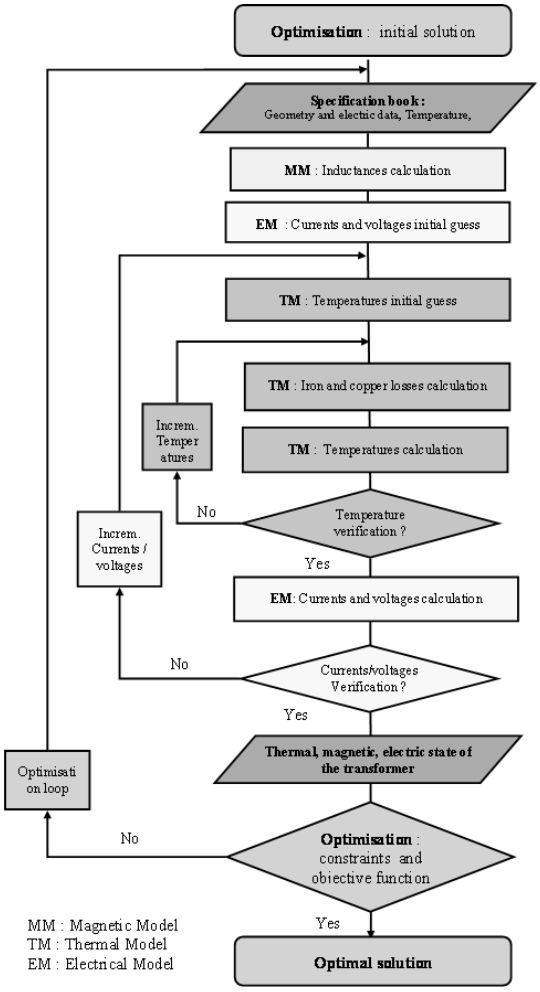

Fig. 7. Flow chart of the optimization

E. Implantation of the optimization procedure

The approach previously described has been implemented in a MATLAB environment (figure 7).

The initial solution of the optimization is based on classical rules of art and a manual design. This solution partly defines the initial specification book of the model, that encompass external data such the external diameter or the airgap height.

The three models, described above, are linked through an iterative unidirectional research algorithm based on the proper estimation of two variables :

- the temperature of the windings that induces on the copper losses through the winding resistance
- the currents and voltages of the electrical that depends on the calculation of the inductances and resistances and consequently on this of the winding temperature.

The optimizer is the MATLAB function ”fmincon” that allows a versatile research.

IV. Design results

The foregoing analytical models and optimization process have been applied to the replacement of the gliding contacts of the WRSM operating as a starter-generator and described in [3].

A. Specification book of the rotary transformer

The rotary transformer is fixed between the WRSM rotor and its front bearing and is consequently subject to the same automotive

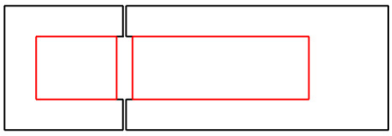

Fig. 8. Cross section (half) of the optimised rotary transformer : internal core (left) secondary rotating part and external core (right) static primary

constraints :

- Low size of the rotary transformer (the total width is the objective function to be minimized)
- Voltage limited by the battery : up to 36 V in Motor mode and up to 42 V in generator mode depending on the battery technology
- High temperature of the environment : 125 °C.
- High efficiency : the efficiency of the transformer (alone) is fixed at least to 80%
- Vibration, mechanical stress and acyclism lead to define a minimum airgap height of 0.5 mm

As seen in subsection III-D.2, the transformer design software incorporates a lumped parameter thermal model that allows to set maximum temperature limit for the primary and secondary windings of 170°C rather than setting current density as an indirect surrogate for these thermal limits.

Moreover, the electrical frequency has been fixed to 800 Hz as it is the limit of validity of the iron loss model.

The primary peak current has been restricted to 115 A peak due to the electronic switch requirements.

The main characteristics of the rotary transformer specification book are summarized in table I.

Parameters	Value
External radius	127.5 mm
Internal radius	67.0 mm
Airgap	0.5 mm
Load power	800 W
Load resistance	1.5 Ω
Load current	23 Adc
Battery voltage	36 Vdc
External air temperature	125 °C
Iron sheet quality	M 47
Frequency	800 Hz

TABLE I
SPECIFICATION BOOK OF THE TRANSFORMER

B. Optimization results

The optimization is performed with the MATLAB constrained SQP optimizer. The width of the transformer is used as the optimization criterion. Several optimizations have been carried out with different initial solutions to ensure the robustness of the solution.

Table II provides several key metric and performance characteristics of the optimal rotary transformer.

1) Finite element analysis results: Electromagnetic FEM is first used to confirm the transformer parameters calculated with the lumped parameter network and to estimate the primary and secondary peak currents. In the FEM software, the transformer is modelled with a primary voltage sinusoidal source and a secondary that consists of a bridge rectifier associated with an R-L load corresponding to the rotor of the WRSM. The FEM software used is FLUX 2D from Cedrat.

Parameters	Value
Total width	19.6 mm
Primary slot height	28.8 mm
Secondary slot height	13.7 mm
Slot width	9.9 mm
Primary turn number	5
Secondary turn number	16
Transformer efficiency (alone)	90.4%
DC-DC converter efficiency	78.8%

TABLE II
OPTIMIZATION RESULTS

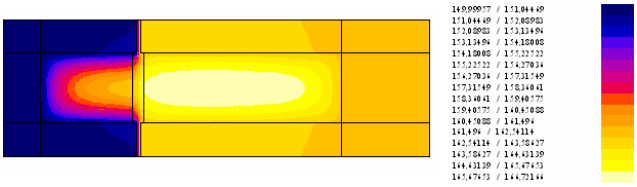

Fig. 9. Thermal map of the rotary transformer

Table III shows the FEM-predicted and lumped parameter flux density corresponding to several parts of the rotary transformer. The maximum difference occurs for the primary yoke lower part with 7%.

Flux density	Lumped model	FEM
Primary yoke upper part	0.13 T	0.10 T
Primary leg	0.33 T	0.32 T
Secondary yoke lower part	0.26 T	0.28 T
Secondary leg	0.25 T	0.26 T

TABLE III
FLUX DENSITY OF THE ROTARY TRANSFORMER

One of the underlying reasons for this difference is that the primary peak current of the estimated FEM software is 5% lower than the lumped parameter network wheras the WRSM rotor load current is 7% lower. This slight difference partly results from the diode model used in the FEM software.

Parameters	Lumped model	FEM
Primary peak current	113.6 A	108.0 A
Load current	23 Adc	21.5 Adc

TABLE IV
CURRENT OF THE ROTARY TRANSFORMER

The FEM software FLUX 2D is also used to calculate the internal transformer temperatures and to verify that it falls within safe limit area (170°C) for the worst case operating point (low rotation speed and external air temperature of 125°C). The hottest point among all the entries is the primary winding with a temperature that approaches the maximum temperature limit. The two models show a good agreement of 97%.

2) Performances analysis: As indicated in table II, the rotary transformer achieves its primary goal of offering a contactless power transmission system with the same compactness as the gliding contacts system owing to a width (without diode rectifier) of 19.6 mm compared to 35 mm for the WRSM prototype. It is important to note

Temperature	Lumped model	FEM
Primary yoke	168°C	163°C
Primary winding	170°C	167°C
Secondary yoke	151°C	151°C
Secondary winding	157°C	160°C

TABLE V
TEMPERATURE OF THE ROTARY TRANSFORMER

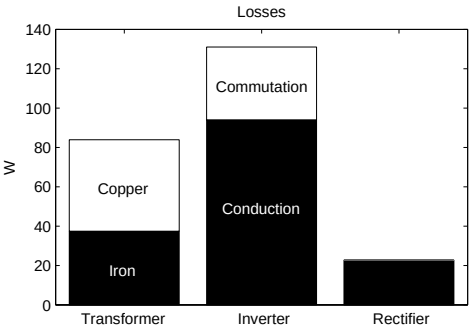

Fig. 10. Comparison of losses of the transformer

that gliding contacts for claw pole alternators rotor supply are 30 mm long for an injected power of less than 100 W.

The performances results of Table III and Table IV reveal first that thermal constraints condition by far the design of the rotary transformer with a temperature of the primary winding of 170°C which is the maximum allowable temperature.

Conversely, the maximum flux density of the iron silicon materials is below 0.35 T which is five time less than its saturation flux density. The underlying reason of this flux density level is the electrical frequency of 800 Hz resulting in a reduction of the magnetizing current compared with a classical 50 Hz transformer.

The choice of the magnetic material must consequently be focused both on the material thermal properties including the iron losses and its mechanical properties instead of its flux density level. Stated differently, a material with poorer flux density saturation level but higher thermal conductivity and yield stress perfectly suits to this application.

However, the improvements of the rotary transformer must be weighed against disadvantages that are apparent in the table IV, namely the primary current of 113 A peak and the total efficiency of 78.8%.

The primary current is first due to the low magnetizing inductance and by extension the airgap height which is compulsory to ensure a contactless system. Then, this rotary transformer is a current step up transformer because of the secondary bridge rectifier associated with the fact that the WRSM rotor windings have been designed with a 36 Vdc voltage (battery supply) [3].

It is interesting to note that the total efficiency for the rotary transformer is 78.8 % (inverter and rectifier included) whereas it is roughly 90 % for the gliding contacts system. As the bar chart of figure 10 shows, this difference mainly results from the inverter losses and especially the conduction losses (94 W) and, as mentioned before, from the primary current of 113 A peak. It's all the more so as the gliding contacts converter is a simple buck step down converter (without bridge rectifier) with only one switch and associated free wheeling diode where a maximum current equal to the WRSM maximum current (23 A) flows.

V. Conclusion

This investigation has used a wound rotor synchronous machine operating as an integrated starter generator to provide valuable insight into the strengths and limitations of replacing the gliding contacts of the machine with an iron silicon axial rotary transformer.

The proposed design method of rotary transformer encompasses non linear electromagnetic, thermal and electrical models and offers a precision better than 7% compared with FEM thermal and magnetic software FLUX 2 D. These coupled models associated with a SQP optimization algorithm demonstrate that the rotary transformer is a good challenger for the gliding contacts system in term of width and also lifetime which is a key concept for integrated structures.

The design also reveals that the choice of magnetic material for such application mainly relies on the thermal conductivity, losses properties and mechanical strength of the material instead of the saturation flux density level. In this way, new materials like soft magnetic composites could replace the silicon steel.

Nevertheless, the designed rotary transformer suffers from a high primary current and as a result a low efficiency of 79% compared with a classical gliding contacts system. This disadvantage will be overcome in a future work by first optimizing both the WRSM rotor winding structure along with the rotary transformer in order to minimize the primary current for a fixed transformer width.

References

[1] J. Miller, V. Stefanovis, V. Ostovic, J. Kelly, *Design consideration for an automotive integrated starter generator with pole phase modulation*, IAS conference,Oct. 2001

[2] G. Friedrich, L. Chédot, J.M. Biedinger, *A comparison of two optimal designs for integrated starter generator applications*, ICEM 2002 - Bruges, Belgique

[3] G. Friedrich, A. Girardin, *Optimal control for wound rotor synchronous starter generator*, IEEE IAS 2006, Tampa, Floride, Oct. 2006

[4] S; MacMinn, W. Jones, *A very high speed switched reluctance starter generator for aircraft engine applications*,in Proc NAECON 89, pp. 1758-1764, May 1999

[5] Wm. T. McLyman, *Transformer and Inductor design Handbook*, Third edition, Book, Marcle Dekker, Inc, 2004

[6] G. Roberts, A.R Owens, P.M Lane, M.E. Humphries, R.K. Child, F. Bauder, J.M. Gavira, *A contactless transfer device for power and data*, Proc. IEEE 1996 Aerospace Applications Conference, Aspen, Colorado, pp 333-345, 3-10 Feb. 1996

[7] G. Roberts, A.R Owens, P.M Lane, M.E. Humphries, R.K. Child, F. Bauder, J.M. Gavira, *A contactless transfer device for power and data* Proc. IEEE 1996 Aerospace Applications Conference, Aspen, Colorado, 333-345, 1996

[8] M. Perottet, *Transmission électromagnétique rotative d'énergie et d'information sans contact*, Thèse d'Université, Ecole Polytechnique Fédérale de Lausanne, Suisse, 2000

[9] J. M. Biedinger, J.-P. Vilain, *Dimensionnement des actionneurs électriques alimentés à fréquence variable sous faible tension*, European Physical Journal Applied Phyics **3**, 101-118, 1998

[10] H. C. Roters, *Electromagnetic Devices*, John Wiley & Sons, 1941

[11] G. Bertotti., *General properties of Power Losses in Soft Ferromagnetic Materials*, IEEE Trans. on Magnetics, vol. 24, n° 1, pp. 621-630, Jan. 1988.

[12] D. Roye, *Modélisation thermique des machines électriques tournantes-Application à la machine à induction*, thesis, Institut National Polytechnique de Grenoble, 1983

[13] B. Renard, *Etude experimentale et modélisation thermique du comportement d'une machine électrique multi-fonction*, thesis, ENSMA, Poitiers, 2003

[14] F.P Incropera, D.P. Dewitt, *Introduction to heat transfer*, Third Edition, John Wiley and Sons, 1996